

Supporting Information

Fabrication, performance and mechanism of MgO meso- /macroporous nanostructures for simultaneous removal of As(III) and F in groundwater system

Panpan Gao^a, Xike Tian^{b}, Chao Yang^b, Zhaoxin Zhou^b, Yong Li^b, Yanxin Wang^{a**},
Sridhar Komarneni^c*

^aSchool of Environmental Studies, China University of Geosciences, Wuhan 430074,
P.R. China.

^bFaculty of Materials Science and Chemistry, China University of Geosciences,
Wuhan 430074, P. R. China.

^cDepartment of Ecosystem Science and Management, Materials Research Institute,
Materials Research Laboratory, The Pennsylvania State University, University Park,
PA 16802

Corresponding Author:

* E-mail: xktian@cug.edu.cn. Tel /Fax: +86-27-67884574.

** E-mail: yx.wang@cug.edu.cn. Tel / Fax: +86-27-87481030.

Experimental Section

1) One-site Langmuir model

$$q_e = \frac{q_{\max} b c_e}{1 + b c_e}$$

Where q_e (mg/g) and c_e (mg/L) are the adsorbed amount and concentration at equilibrium, respectively; b (L/mg) represents the Langmuir constant that relates to the affinity of binding sites; q_{\max} (mg/g) is the maximum adsorption capacity.

2) Two-site Langmuir model

$$q_e = \frac{q_1 b_1 c_e}{1 + b_1 c_e} + \frac{q_2 b_2 c_e}{1 + b_2 c_e}$$

Where q_1 and q_2 (mg/g) are the maximum uptake at high and low energy sites, respectively; b_1 and b_2 (L/mg) represent the Langmuir constants that relate to the affinity of binding sites.

3) Freundlich model

$$\ln q_e = \ln k_F + \frac{1}{n} \ln c_e$$

Where K_F and n are the Freundlich constants, which represent the adsorption capacity and the adsorption strength, respectively. The magnitude of $1/n$ quantifies the favorability of adsorption and the degree of heterogeneity of the adsorbent surface.

4) Pseudo-first-order model

$$\ln (q_e - q_t) = \ln q_e - k_1 t$$

Where q_e (mg/g) and q_t (mg/g) are the amounts of anions adsorbed on MgO at equilibrium and time t (min), respectively; k_1 (min^{-1}) is the rate constant of the pseudo first-order kinetic model.

5) Pseudo-second-order model

$$\frac{t}{q_t} = \frac{1}{k_2 q_e^2} + \frac{t}{q_e}$$

Where k_2 ($\text{g mg}^{-1} \text{min}^{-1}$) is the rate constant of pseudo-second-order kinetic model.

6) Elovich model

$$q_t = \frac{1}{\beta} \ln(\alpha\beta) + \frac{1}{\beta} \ln t$$

Where α and β are Elovich constants, which are related to adsorption rate and surface coverage, respectively.

7) Intra-particle diffusion model

$$q_t = k_d t^{1/2} + I$$

Where I (mg/g) is the intercept and k_{di} ($\text{mg g}^{-1} \text{min}^{-0.5}$) is the rate constant of the i line portion.

List of Tables :

Table S1. Isotherm parameters for single adsorption of As(III) and F on MgO samples.

Table S2. Kinetic parameters for single adsorption of As(III) and F on MgO nanostructures.

Table S3. Intra-particle diffusion model parameters for single adsorption of As(III) and F on MgO nanostructures.

Table S4. O1s of MgO nanostructures before and after As(III)/F adsorption.

List of Figures:

Figure S1. Effect of contact time on (a) As(III) and (b) F adsorption onto MgO nanostructures at different MgO loadings.

Figure S2. Effect of initial solution pH on (a) As(III) and (b) F adsorption of MgO nanostructures.

Figure S3. Effect of coexisting anions on (a) As(III) and (b) F adsorption of MgO nanostructures.

Figure S4. (a) XPS wide scan spectra of MgO before (the MgO after immersion in water for 24 h) and after adsorption of As(III) and F. (b) Partial spectra of MgO before and after As(III) adsorption. (c) F1s spectra of MgO after F adsorption. High-resolution O1s spectra of MgO (d) before and after adsorption of (e) As(III) and (f) F.

Figure S5. SEM images of MgO sample (b) before and (a) after adsorption in practical groundwater treatment.

Figure S6. Variation of the removal rates of As(III) and F on MgO in successive cycles in practical groundwater treatment.

Table S1. Isotherm parameters for single adsorption of As(III) and F on MgO samples

Anions	$q_{e,exp}$ ($mg \cdot g^{-1}$)	One-site Langmuir			Two-site Langmuir					Freundlich			
		q_m ($mg \cdot g^{-1}$)	b	R^2	q_1 ($mg \cdot g^{-1}$)	q_2 ($mg \cdot g^{-1}$)	q_m ($mg \cdot g^{-1}$)	b_1	b_2	R^2	k_F	1/n	R^2
As(III)	532.098	540.90	0.15	0.983	271.45	271.45	542.90	0.15	0.15	0.980	112.34	0.41	0.78
F	202.8	206.80	0.03	0.960	207.92	82.75	290.67	0.004	0.31	0.999	29.95	0.34	0.989

Table S2. Kinetic parameters for single adsorption of As(III) and F on MgO nanostructures

Anions	Dosage (g•L ⁻¹)	q _{e,exp} (mg•g ⁻¹)	Pseudo-first-order			Pseudo-second-order			Elovich model		
			k ₁ (min ⁻¹)	q _{e,cal} (mg•g ⁻¹)	R ²	k ₂ (g•mg ⁻¹ •min ⁻¹)	q _{e,cal} (mg•g ⁻¹)	R ²	α	β	R ²
As(III)	0.5	12.453	0.087	11.867	0.905	0.302	12.214	0.998	12.287	0.672	0.773
	0.75	9.085	0.159	8.654	0.873	0.726	8.895	0.999	984.752	1.403	0.694
	1	6.875	0.154	6.691	0.968	0.509	6.837	0.999	1458.671	1.934	0.722
F	0.5	18.865	0.067	18.414	0.891	0.562	18.146	0.997	19.382	0.394	0.668
	1	19.062	0.153	18.819	0.990	2.205	18.985	1	9038	0.737	0.536

Table S3. Intra-particle diffusion model parameters for single adsorption of As(III) and F on MgO nanostructures

Dosage (g•L ⁻¹)	Anions	Intra-particle diffusion								
		k _{d1} (mg/(g•min ^{1/2}))	I ₁	R ₁ ²	k _{d2} (mg/(g•min ^{1/2}))	I ₂	R ₂ ²	k _{d3} (mg/(g•min ^{1/2}))	I ₃	R ₃ ²
0.5	As(III)	1.056	3.778	0.895	0.354	8.654	0.905	0.031	12.156	0.750
	F	3.390	-2.079	0.989	0.463	14.188	0.850	0.022	19.179	0.726

Table S4. O1s of MgO nanostructures before and after As(III)/F adsorption

	Mg-OH,%, 531.47 eV	Mg-O,%, 530.51 eV
MgO-H ₂ O	45.2	50.8
MgO-As(III)	30	27.6
MgO-F	40.2	59.8

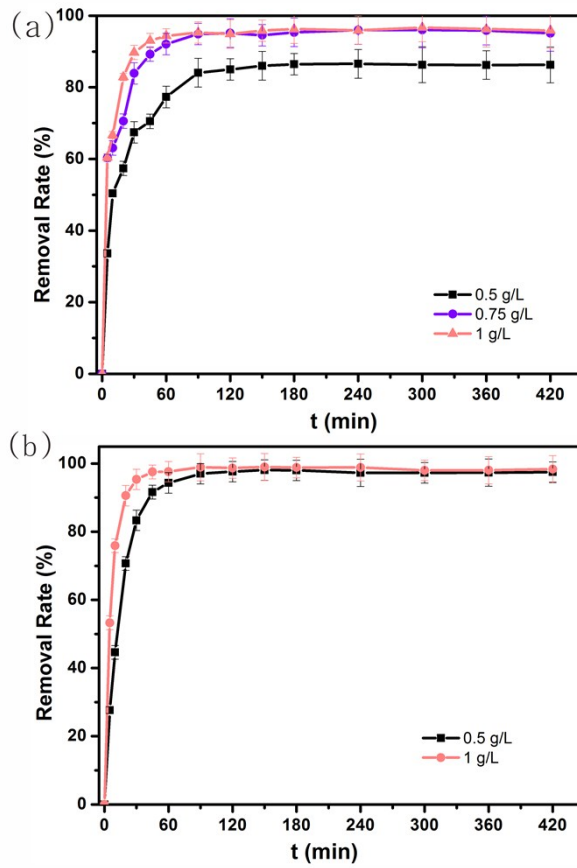


Figure S1. Effect of contact time on (a) As(III) and (b) F adsorption onto MgO nanostructures at different MgO loadings.

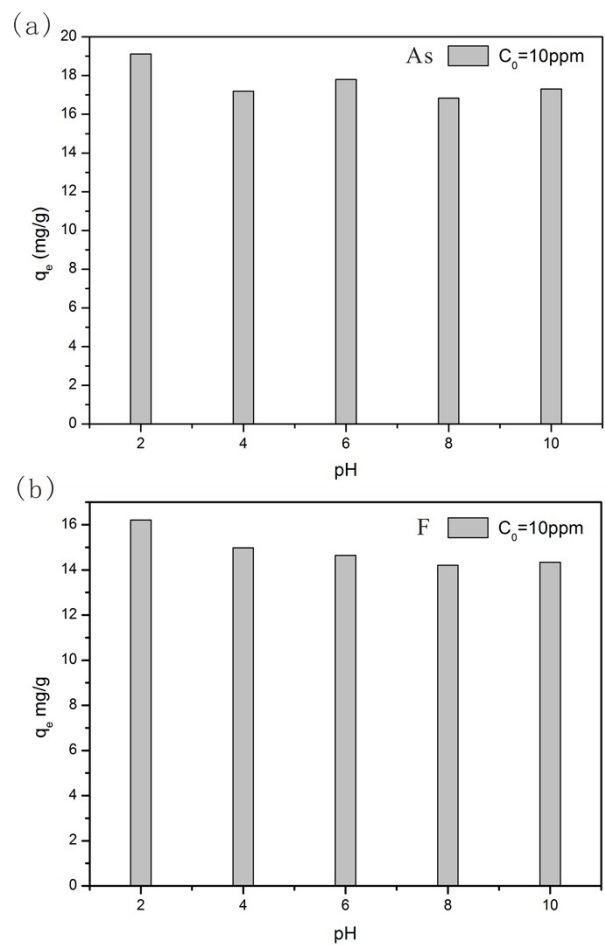


Figure S2. Effect of initial solution pH on (a) As(III) and (b) F adsorption of MgO nanostructures.

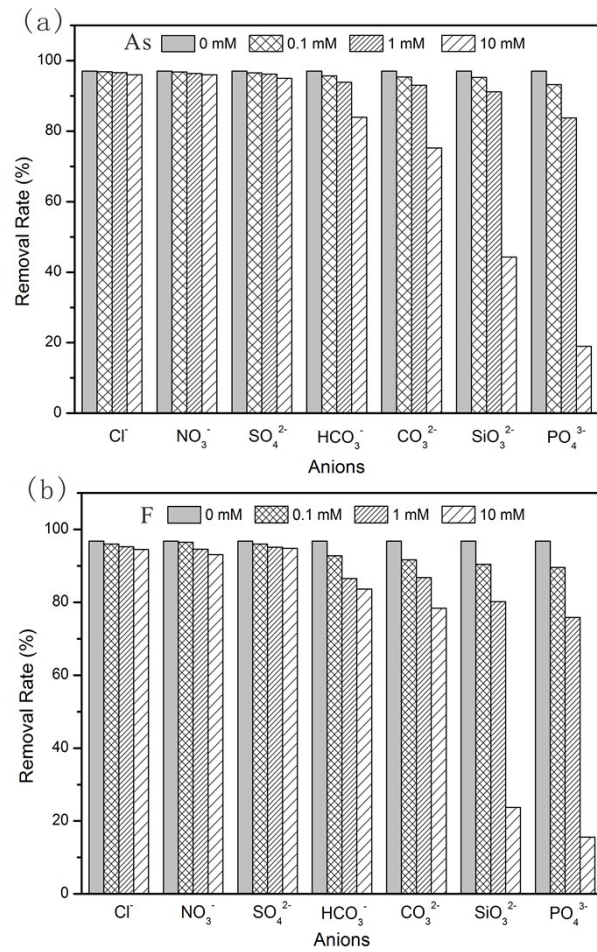


Figure S3. Effect of coexisting anions on (a) As(III) and (b) F adsorption of MgO nanostructures.

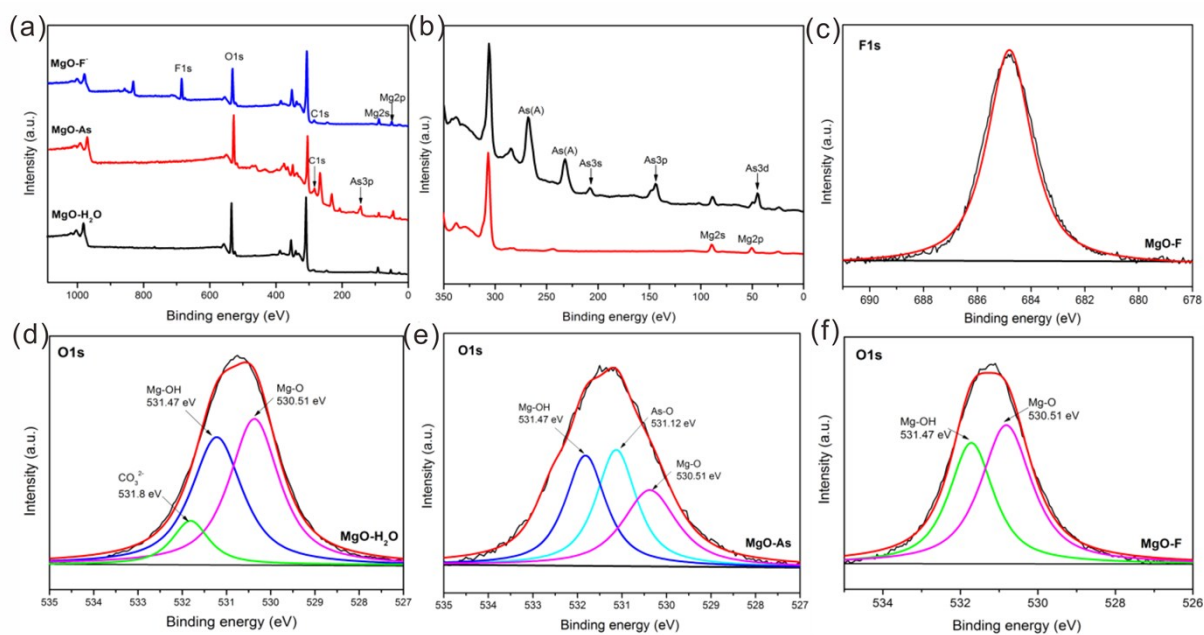


Figure S4. (a) XPS wide scan spectra of MgO before (the MgO after immersion in water for 24 h) and after adsorption of As(III) and F. (b) Partial spectra of MgO before and after As(III) adsorption. (c) F1s spectra of MgO after F adsorption. High-resolution O1s spectra of MgO (d) before and after adsorption of (e) As(III) and (f) F.

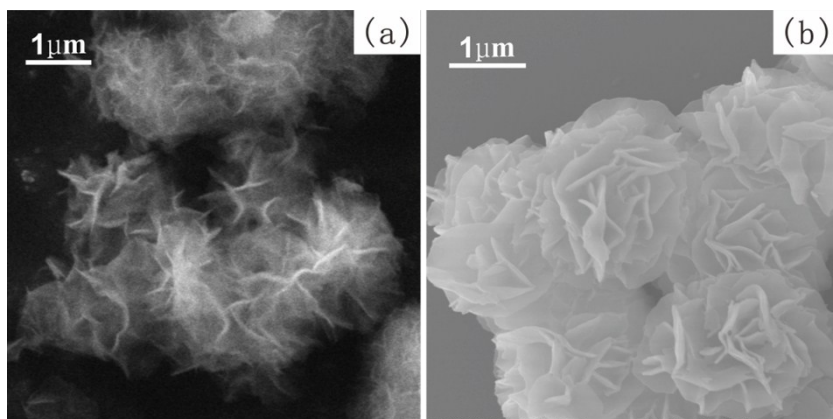


Figure S5. SEM images of MgO sample (b) before and (a) after adsorption in practical groundwater treatment.

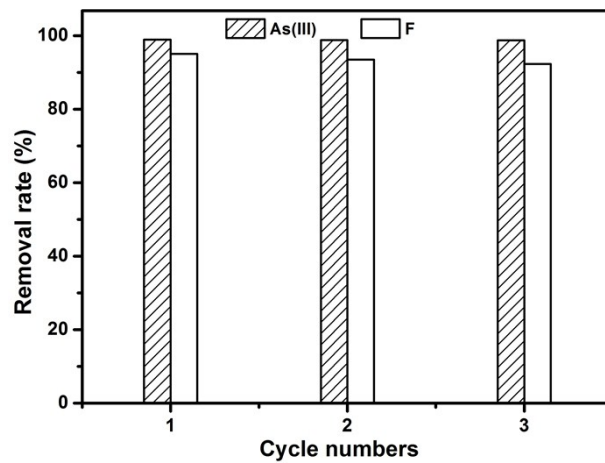


Figure S6. Variation of the removal rates of As(III) and F on MgO in successive cycles in practical groundwater treatment.